Nuclear Inst. and Methods in Physics Research, A 953 (2020) 163194

Contents lists available at ScienceDirect

Nuclear Inst. and Methods in Physics Research, A

journal homepage: www.elsevier.com/locate/nima

Commissioning of the electron injector for the AWAKE experiment

S.-Y Kim [a], S. Doebert [b], O. Apsimon [c], R. Apsimon [d], G. Burt [d,e], M. Dayyani [f], S. Gessner [b], I. Gorgisyan [b], E. Granados [b], S. Mazzoni [b], J.T. Moody [g], M. Turner [b], B. Williamson [c,e], M. Chung [a,*]

[a] Department of Physics, Ulsan National Institute of Science and Technology, Ulsan 44919, Republic of Korea
[b] CERN, Geneva 1211, Switzerland
[c] Manchester University, M13 9PL Manchester, United Kingdom
[d] Lancaster University, LA1 4YW Lancaster, United Kingdom
[e] Cockcroft Institute, WA4 4AD Warrington, United Kingdom
[f] Institute for Research in Fundamental Sciences, 19395-5531, Tehran, Iran
[g] Max Planck Institute for Physics, 80805 Munich, Germany

ARTICLE INFO

Keywords:
Plasma
Wakefield
AWAKE
Electron injector

ABSTRACT

The advanced wakefield experiment (AWAKE) at CERN is the first proton beam-driven plasma wakefield acceleration experiment. The main goal of AWAKE RUN 1 was to demonstrate seeded self-modulation (SSM) of the proton beam and electron witness beam acceleration in the plasma wakefield. For the AWAKE experiment, a 10-meter-long Rubidium-vapor cell together with a high-power laser for ionization was used to generate the plasma. The plasma wakefield is driven by a 400 GeV/c proton beam extracted from the super proton synchrotron (SPS), which undergoes a seeded self-modulation process in the plasma. The electron witness beam used to probe the wakefields is generated from an S-band RF photo-cathode gun and then accelerated by a booster structure up to energies between 16 and 20 MeV. The first run of the AWAKE experiment revealed that the maximum energy gain after the plasma cell is 2 GeV, and the SSM mechanism of the proton beam was verified. In this paper, we will present the details of the AWAKE electron injector. A comparison of the measured electron beam parameters, such as beam size, energy, and normalized emittance, with the simulation results was performed.

1. Introduction to AWAKE

The advanced wakefield experiment (AWAKE) at CERN studies electron beam acceleration in proton beam-driven plasma wakefields [1,2]. The proton beam driver has a momentum of 400 GeV/c, a bunch length of 6–12 cm (RMS), and a transverse beam size of 0.2 mm (RMS). The plasma is generated in a 10-meter-long heated Rubidium-vapor source that can reach plasma densities of the order of $1 \times 10^{14} \sim 1 \times 10^{15}/\mathrm{cm}^3$. The ionization laser has an energy of 450 mJ and a pulse length of 120 fs (FWHM), allowing full ionization of a plasma channel with a radius of 1 mm. The laser pulse and the proton beam co-propagate through the vapor source to create the plasma, and seed the self-modulation within the long proton bunch. The maximum accelerating gradient of the plasma wakefield [3] $E_{max} = m_e w_{pe} c/e$ is determined by the plasma electron density n_e, where m_e is the electron mass, $w_{pe} = \sqrt{n_e e^2/m_e \epsilon_0}$ is the plasma frequency, ϵ_0 is the vacuum permittivity, c is the speed of light, and e is the electron charge. In the case of AWAKE, the nominal plasma density is $7 \times 10^{14}/\mathrm{cm}^3$, and the maximum accelerating gradient is therefore expected to be on the order of GV/m.

An important condition particular to AWAKE for the generation of a high plasma wakefields is the seeded self-modulation (SSM) of the proton beam [4,5]. In the linear plasma wakefield theory, the optimal condition to drive a plasma wakefields is $k_p \sigma_z \cong \sqrt{2}$, where k_p is the plasma wavenumber defined by w_{pe}/c, and σ_z is the RMS bunch length of the drive beam [6]. Therefore, the initial proton beam extracted from the super proton synchrotron (SPS) does not satisfy the condition needed to generate high-gradient wakefields owing to its long bunch length. However, once the long proton bunch has propagated for a distance in the plasma, it splits into micro-bunches that have a length corresponding to the plasma wavelength and meet the condition for driving the high-gradient plasma wakefield [7]. The self-modulation of the proton beam is reliably seeded by the front of the ionization laser, which is placed in the center of the proton beam. The self-modulation of the proton beam density starts from this point, enabling phase stable wakefields.

In the first run of the AWAKE experiment to demonstrate electron beam acceleration through the plasma wakefields, an electron injector

* Corresponding author.
E-mail addresses: steffen.doebert@cern.ch (S. Doebert), mchung@unist.ac.kr (M. Chung).

https://doi.org/10.1016/j.nima.2019.163194
Received 1 November 2019; Received in revised form 27 November 2019; Accepted 28 November 2019
Available online 29 November 2019

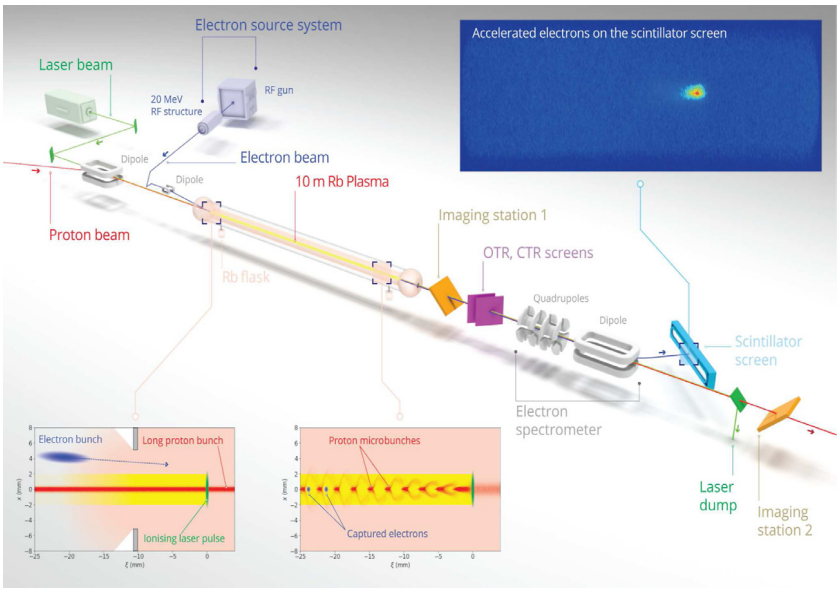

Fig. 1. Schematic of the AWAKE experiment at CERN. The upper right corner shows an example of a beam spot as observed in the spectrometer. The inserts in the lower left corner illustrate the injection conditions and the process of seeded self-modulation.

Table 1
Main parameters of the proton, electron beam and ionization laser for the AWAKE experiment.

Parameters		Value
Proton beam (extracted from SPS)		
Energy		400 GeV
Bunch length σ_z		12 cm
Bunch radius σ_r		0.2 mm
Normalized emittance ϵ_n		3.5 mm mrad
Energy spread σ_δ		0.45%
Electron beam (at the plasma entrance)	Initial set value	Value used for the experiment
Energy	16 MeV	16–20 MeV
Charge	200 pC	140–650 pC
Bunch length σ_z	4 ps	1–4 ps
Bunch radius σ_r	0.25 mm	0.25 mm
Normalized emittance ϵ_n	2 mm mrad	2 mm mrad
Energy spread σ_δ	0.5%	0.5%
Ionization laser (Fiber Ti:Sa)		
Energy		450 mJ
Pulse length σ_z		100–120 fs
Focused spot size σ_r		1 mm

that consists of an S-band RF photocathode gun and a traveling wave booster structure were used to produce electron beams with an energy of 16–20 MeV [8]. The electron beam was then passed through an electron transfer line, and injected into the plasma cell co-propagating with the proton beam and the ionization laser [9,10]. An energy gain of the electron beam in the 10 m plasma source of up to 2 GeV [11] has been demonstrated experimentally. In addition, the SSM phenomenon has been successfully observed and studied by direct measurement of the modulated proton bunch using streak cameras, and by indirect measurement of the proton beam divergence due to the transverse wakefield [12,13]. A schematic of the AWAKE experiment can be seen in Fig. 1 and main parameters of the proton, electron beam and ionization laser can be seen in Table 1.

Details of the electron beam parameters required for electron beam acceleration in the plasma wakefield are summarized in Refs. [14,15]. Since the main goal of the AWAKE RUN 1 experiment was to determine whether the electron beam is accelerated in the proton beam-driven plasma wakefield, the focus was on the matching of the electron beam to the plasma channel containing the wakefields. The biggest constrain was the transverse RMS beam size at the entrance of the plasma cell and therefore the emittance of the electron beam. In order to control the electron beam size and the emittance along the transfer line, and to satisfy the parameters required at the plasma entrance, understanding of the electron injector was essential. Therefore, the main parameters of the electron beam along the electron injector have been measured and compared with the simulations to determine the operational conditions. In this paper, we will present the details of the electron injector. A description of the electron injector and commissioning results such as transverse beam distributions on screens and beam emittance measurements using pepper-pot and quadrupole scan methods will be shown in Sections 2 and 3. A careful comparison of the measurements with the simulation results in order to characterize the operating condition of the electron injector will be presented in Section 4. Finally, the results of the commissioning will be concluded in Section 5.

2. Design and construction of the injector

An electron injector providing adequate beam quality to demonstrate the first proton driven plasma wakefield acceleration experiment was designed and constructed by AWAKE collaborators. The original target parameters for the injector were energy of 16 MeV, a bunch charge of 200 pC, an energy spread below 1%, a bunch length of 4 ps, and an emittance of 2 mm mrad. To achieve these parameters, an RF photo-injector was chosen using a 3 GHz, 2.5-cell RF-gun and a one-meter-long booster structure. The RF-gun including a load-lock system was available at CERN [16], while the booster structure was newly developed for this purpose [17]. The load-lock system enables the use of Cs_2Te cathodes fabricated at CERN with a quantum efficiency of $Qe \sim 10^{-2}$. The laser beam was derived from the main Ti-Sa laser used to ionize and seed the proton beam self-modulation. Consequently, an adequate timing synchronization could be achieved. A small fraction of the initial laser power was frequency tripled to a wavelength of 262 nm and sent with an off-axis mirror on the cathode. The UV-beamline allows users to vary the spot size and energy on the cathode as well as the bunch length as the IR-laser beam has to be compressed before the UV conversion [18]. The RF-gun accelerates the electron bunches to an energy of 5.5 MeV, and then the booster can add a maximum energy of 16 MeV. A single klystron is used to power the gun and

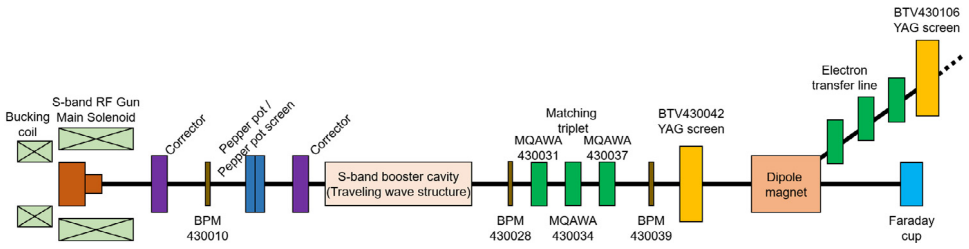

Fig. 2. Schematic electron injector layout emphasizing the location of magnets and diagnostics mentioned throughout the paper.

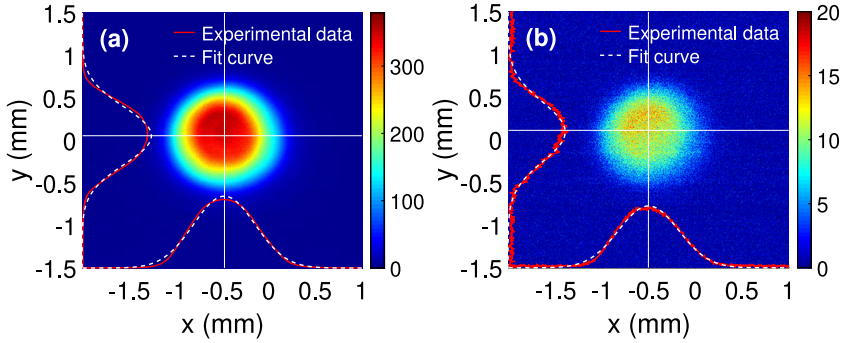

Fig. 3. Initial transverse distribution of the laser at the cathode without an OD filter (a) and with OD filter (b).

the booster structure. A high power wave-guide attenuator and phase-shifter allow for individual phasing and powering of the two structures. A particular challenge for the design and construction was the severe space constraints in the AWAKE experiment. The complete injector has a total length of only 5 m before the beam transport towards the plasma cell starts. The injector was equipped with a number of beam diagnostics as described in more detail in the next section.

3. Beam commissioning results

Fig. 2 shows a schematic view of the electron injector indicating, in particular, the locations of focusing and beam diagnostic elements used in this section. The electron injector consists of an S-band RF photocathode gun and booster structure. The main solenoid and the corresponding bucking coil are placed around the RF gun to control the beam focusing and emittance compensation. Corrector magnets are used to correct the beam trajectory, which can be measured with several strip-line BPM's [19]. A pepper-pot beam diagnostic instrument is used to measure the beam emittance out of the RF-gun, and the screen behind the retractable pepper-pot also allows imaging of the transverse distribution of the beam. A quadrupole triplet behind the booster structure is used to match the beam for further beam transport and for the emittance measurements using the quadrupole scan method at higher energies. A YAG screen (BTV430042) is used to measure the transverse beam distribution. The electron beam charge at the end of the injector is measured by a Faraday-cup with high precision. The first dipole magnet of the following transport line together with a second screen also serves as a spectrometer to measure the beam energy and energy spread. During the commissioning, as many beam parameters as possible were measured so that they can be used as input parameters for simulations.

First, the initial transverse distribution of laser pulse was measured using the so-called virtual cathode camera. This camera images a fraction of the laser beam in similar imaging conditions as the laser pulse sent to the cathode. The laser energy can be varied with optical density (OD) filters to adjust the final beam charge. The beam charge during the commissioning reported here was measured as 140 ± 10 pC. The initial transverse distribution of the laser is shown in Fig. 3. Fig. 3(a) shows the case without the OD filter, which is used to enhance the UV imaging. The RMS transverse beam size can be determined as $\sigma_x = 0.33$ mm in the horizontal plane, and $\sigma_y = 0.34$ mm in the vertical plane. In the experiment, however, an OD filter was used to reduce the beam charge, which resulted unfortunately in a poorer quality image of the virtual cathode as can be seen in Fig. 3(b). The transverse size of the laser obtained by analyzing this image appears slightly reduced owing to the cut-off of the laser energy, and we found that σ_x and σ_y are 0.27 mm. The smaller values were used for the particle tracking simulations later on. The bunch length of the electron beam was not measured during the experiment. Previous measurements of the UV laser beam suggested a laser pulse length of $\sigma_z = 2.2$ ps (FWHM 5.2 ps).

The energy of the electron beam out of the RF gun was calculated by measuring the position of the beam at the pepper-pot screen while scanning the first corrector magnet, as no actual spectrometer is available after the gun. The electron beam momentum out of the RF-gun was determined to be 5.8 MeV/c, which corresponds to a nominal energy of 5.3 MeV. However, as this measurement has a much lower precision compared to that of a real spectrometer magnet, we estimated the error of the electron beam energy calculation to be about 10%. The energy of the electron beam after the traveling wave structure was measured using the first dipole magnet in a proper spectrometer setup. The momentum of the electron beam after acceleration was determined as 18.5 MeV/c with an error of 0.3%.

To optimize the operating conditions of the electron injector during commissioning, scans of the main solenoid around the RF-gun responsible for emittance compensation have been performed. Beam sizes and emittances have been measured before and after the booster structure as a function of the solenoid current. First, the transverse beam size of the electron beam was measured on the pepper-pot screen. Fig. 4(a) depicts the beam size and normalized emittance as a function of the solenoid current. The minimum beam sizes σ_x and σ_y at the pepper-pot screen are 0.47 mm and 0.38 mm for a solenoid current of 185 A. We found during the commissioning that it was very difficult to obtain reliable and reproducible emittance measurements with our pepper-pot setup. The cause of this observation is still under investigation. At this point, we tend not to rely on these measurements. We will come back to that issue in the simulation section.

In addition to the measurement at the pepper pot screen, the beam size and normalized emittance after the traveling wave structure

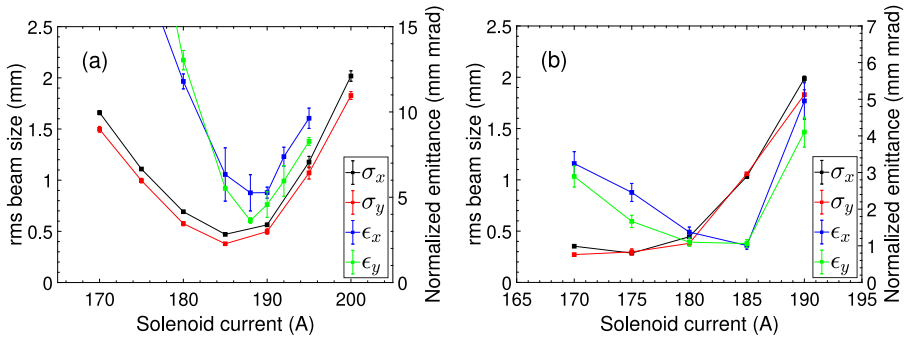

Fig. 4. Measured transverse beam size and normalized emittance of the electron beam at the pepper-pot (a) and BTV 430042 screen (b).

have been measured. This time a well-established quadrupole scanning method was used as the beam is no longer space charge dominated. The beam size was measured at the BTV430042 screen, while the normalized emittance was determined from a quadrupole scan by varying the magnetic field of the center quadrupole of the triplet (MQAWA430034). Fig. 4(b) shows the beam size at the screen (BTV430042) and the normalized emittance as a function of the solenoid current. The minimum beam size was found at a solenoid current of 175 A: σ_x is 0.29 mm and σ_y is 0.30 mm. The minimum normalized emittance, on the other hand, was found at a solenoid current of 185 A, which is 1.0 mm mrad in both the horizontal and the vertical plane. Relative error of the emittance in Fig. 4(b) was determined as follows: When using the quadrupole scan method, beam size was measured ten times at each quadrupole magnet strength. Then, the polynomial curve fitting was performed to find ten sets of emittance values. The relative error of the emittance in the range of the solenoid current was about 10%.

In the next section, we will show a comparative analysis of experimental measurements with the results obtained from the simulations.

4. Comparison with simulations

To compare measured beam parameters with the simulation results, particle tracking was performed mainly using the ASTRA [20] code. The cathode material used in AWAKE is Cs_2Te, and the characteristic parameters of the electron beam emitted from the cathode such as the thermal emittance and momentum distribution can be defined in terms of the Fermi–Dirac distribution [21,22]. In ASTRA, the momentum distribution, and thermal emittance of the initial beam at the cathode are defined as follows [23]:

$$\sigma_{p_x} = \sigma_{p_y} = \sqrt{\frac{E_{photon} - \phi_{eff}}{3m_e c^2}}, \tag{1}$$

$$\sigma_E = \frac{E_{photon} - \phi_{eff}}{3\sqrt{2}}, \tag{2}$$

$$\epsilon_{x,y} = \sigma_{x,y}\sqrt{\frac{E_{photon} - \phi_{eff}}{3m_e c^2}}, \tag{3}$$

where $\sigma_{p_{x,y}}$ is the RMS value of the transverse momentum, E_{photon} is the photon energy of the laser, ϕ_{eff} is the effective work function of the cathode material, σ_E is the energy spread, and $\epsilon_{x,y}$ is the thermal emittance.

Through the equations above and Ref. [22], the transverse momentum and energy spread are determined only by the photon energy of the laser and the work function of the cathode material, regardless of the spatial distribution type of the laser. As the momentum distribution is determined by E_{photon} and ϕ_{eff} irrespective of the laser shape, the initial beam distribution measured at the cathode (see previous section) was used as an input to the simulation. As can be seen in Fig. 3(b), the distribution is not fully symmetric. To perform the simulations, we converted the measured image into a transverse input distribution suitable for simulations. For the longitudinal components, a distribution generated by ASTRA was used assuming a Gaussian laser pulse shape. For the simulations, as we do not have a real bunch length measurement, we studied three values: 2.2 ps as indicated by previous UV laser measurements and shorter beams with 1.0 ps and 1.5 ps bunch lengths for comparison.

The RF fields of the RF gun were overlaid with the magnetic fields of the solenoids. The maximum accelerating gradient was set to be 79.6 MV/m to obtain the measured beam energy of 5.3 MeV out of the RF gun. At 1.6 m, a traveling wave structure (booster structure) was placed to increase the beam energy to match the measured value of 18.1 MeV; thus its accelerating gradient was 17.8 MV/m. In the ASTRA simulation, a full 3D field map of the booster structure obtained from CST was used, while the field map of the RF gun was determined by the 1D axial electric field owing to a lack of 3D data. The phase of the gun was checked to achieve the maximum energy gain, nominally corresponding to the smallest emittance as well. Therefore, the beam launch phase was approximately 30° off crest in the simulations. In the experiment, we tried to minimize the emittance by varying the phase of the gun and solenoid current around the nominal working point. The booster structure was set to on-crest acceleration as optimized for maximum energy in the experiment.

Solenoid scans were simulated with bunch lengths of 1.0 ps, 1.5 ps, and 2.2 ps. The simulation results together with the measured data are shown in Fig. 5, upper plots for the pepper-pot screen and the lower plots for the BTV 430042 screen. In this case, misalignment of the RF structure and solenoid magnet were not considered. One can see that the slopes of the beam size scans match better with shorter bunch length cases on both screens. This results indicate that the bunch length might have been shorter than 2.2 ps as indicated by previous UV measurements. At the pepper-pot screen, the minimum beam sizes σ_x and σ_y for the case of 1.0 ps bunch length are 0.32 mm and 0.31 mm; furthermore, the minimum values of the normalized emittance are 0.80 mm mrad in the horizontal plane and 0.78 mm mrad in the vertical plane. In addition, the minimum beam sizes σ_x and σ_y at the BTV430042 screen are 0.48 mm and 0.44 mm, and the minimum values of the normalized emittance are very similar to the values at the pepper-pot screen. However, the shape of the scan for the emittance measurements does not correspond well with the simulations. The emittance determination using the pepper-pot data seems to fail because the larger measured values do not agree with the simulations, while the measurements further downstream of the beam line using the quadrupole scan method seem to match well with the simulation results, at least for the minimum values. Therefore, at this point we concluded that the pepper-pot results are not very reliable. The reason for this is still under investigation, and there are hints that the location and dimensions of our device are not optimal [24].

During the experiments, the machine operation and in particular the beam alignment were optimized for the minimum emittance values at 185 A, as these beams have been used for the plasma wakefield

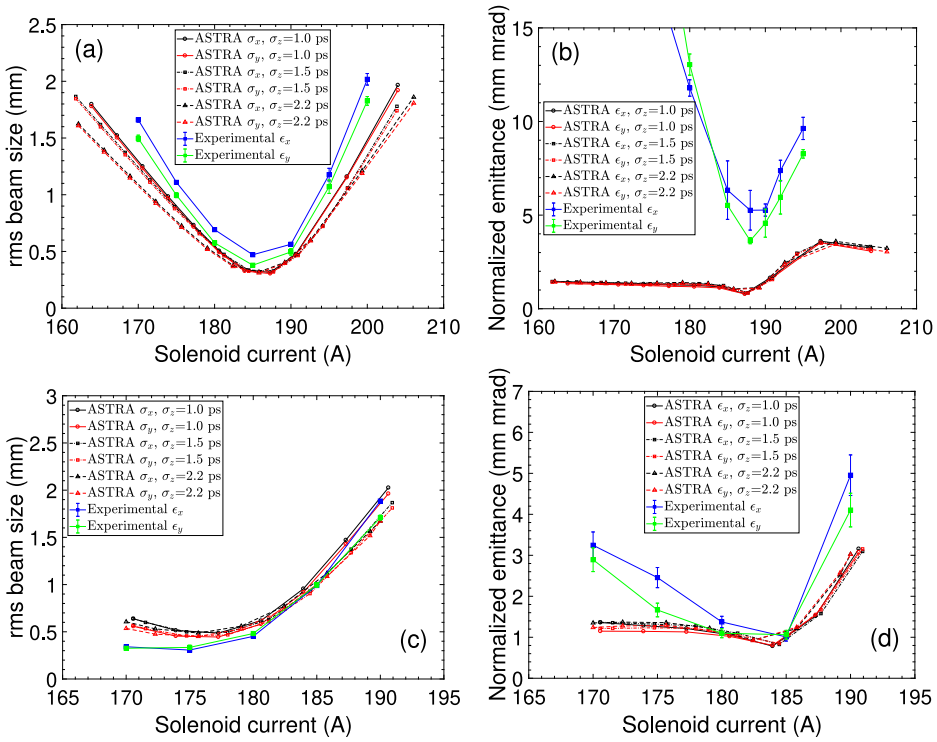

Fig. 5. Transverse beam size and normalized emittance obtained from the ASTRA simulation at the pepper-pot screen (a, b) and BTV430042 screen (c, d) without misalignment.

acceleration experiments. The alignment of the beam was not corrected during the scan. Therefore, we suspect misalignment of the beam due to steering of the solenoid magnet is responsible for the particular shape of the emittance measurements. Particle tracking simulations were used again to study possible offsets of the booster structure and the solenoids, as we had some experimental hints from the beam trajectory data that this might have been the case.

Various offsets of the main solenoid and the booster structure have been studied using ASTRA with 3D space charge calculations and a 3D field map for the booster structure. We found that the measurements are best described assuming a relatively big offset of the booster structure only. Fig. 6 shows a comparison of the experiment data and the simulation results obtained for a −4.5 mm offset at the entrance of the booster structure. In this simulation, a 1.5 ps bunch length was used. Both the emittance and the spot size show good qualitative agreement for these misalignment assumptions.

The emittance growth seen in the simulations is attributed to an RF kick within the input coupler of the booster structure due to its not perfectly compensated RF fields. Phase space distortion due to the asymmetric field is illustrated in Fig. 7, where the top row shows the horizontal phase space at the input coupler of the booster structure obtained from an on-axis simulation, while the bottom row images are with the booster structure offset. One can see that the momentum distribution of the on-axis case is concentrated in the center. In the case with a large beam offset, simulation results reveal that the momentum distribution is distorted with respect to the core, which leads to emittance growth. However, for well-focused beams at the entrance of the booster (solenoid currents of 180 and 185 A), the effect is much smaller, and the emittance growth is not significant.

In a second beam commissioning campaign, the misalignment of the beam in the booster structure and the question of the not well-known bunch length were addressed. The original misalignment of the solenoids could not be solved, so we corrected the beam at the entrance of the booster structure for each solenoid setting using a pair of corrector magnets when taking data. In addition, as the UV pulse shape and length were not clearly determined during the last measurement, UV pulse measurements using a streak camera were performed again. Unfortunately, it was not possible to obtain reliable data from direct bunch length measurements using light from an OTR screen on the streak camera. The intensity arriving at the streak camera was simply not high enough.

The transverse beam distribution and charge of the beam were slightly different from those in the first campaign. Therefore, the following inputs were used for the simulations. Fig. 8 shows the measured transverse beam distribution at the cathode and the measured longitudinal profile of the UV laser pulse. The initial beam size is slightly changed compared to that in Fig. 3(b). Beam sizes σ_x and σ_y are both 0.25 mm. The measured beam charge at the Faraday cup was 150 pC. In the case of the UV measurement, it was confirmed that the RMS UV pulse length was 1.5 ps. In addition, one can see that there is a secondary pulse behind the main pulse, but it is negligible, as the amplitude is very small compared to the main pulse. This afterpulse was not taken into account in the simulations. Even though the simulation results with a 1.5 ps bunch length did not perfectly match with the experimental data indicated in Fig. 5, it was confirmed that the measured bunch length is shorter than that assumed previously.

Using the new measured inputs, the ASTRA simulations were performed again. The booster structure gradient was slightly changed to obtain the experimentally measured 18.8 MeV/c momentum value in the simulation. This time, we obtained a good agreement between simulations and measurements, confirming the assumptions concluded from the analysis of the first measurement campaign. The measured emittance values obtained from quadrupole scans and the simulation results are compared in Fig. 9. The emittance value obtained from the simulation and the experiment are 0.74 mm mrad and 0.70 mm mrad, respectively. In addition, the overall emittance of the beam was reduced owing to a better and more careful setup of the beam.

5. Conclusions

The electron injector for the AWAKE experiment was successfully constructed and commissioned. It enabled successful demonstration of the first ever proton beam-driven plasma wakefield experiments.

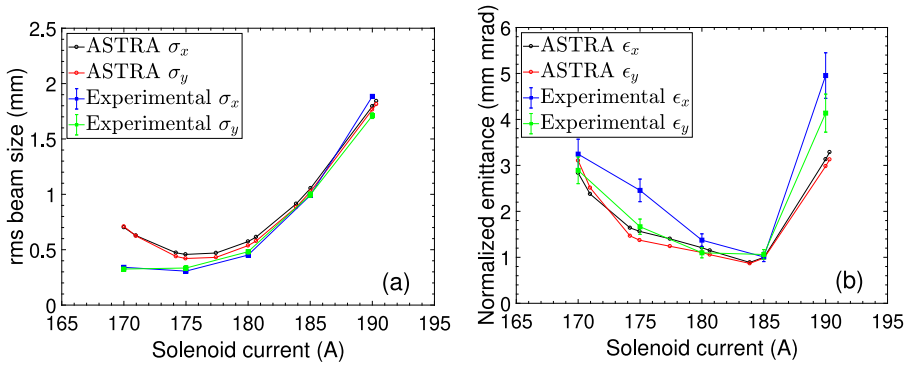

Fig. 6. Comparison of the transverse beam size (a) and normalized emittance (b) at BTV430042 screen taking into account a misalignment of the booster structure.

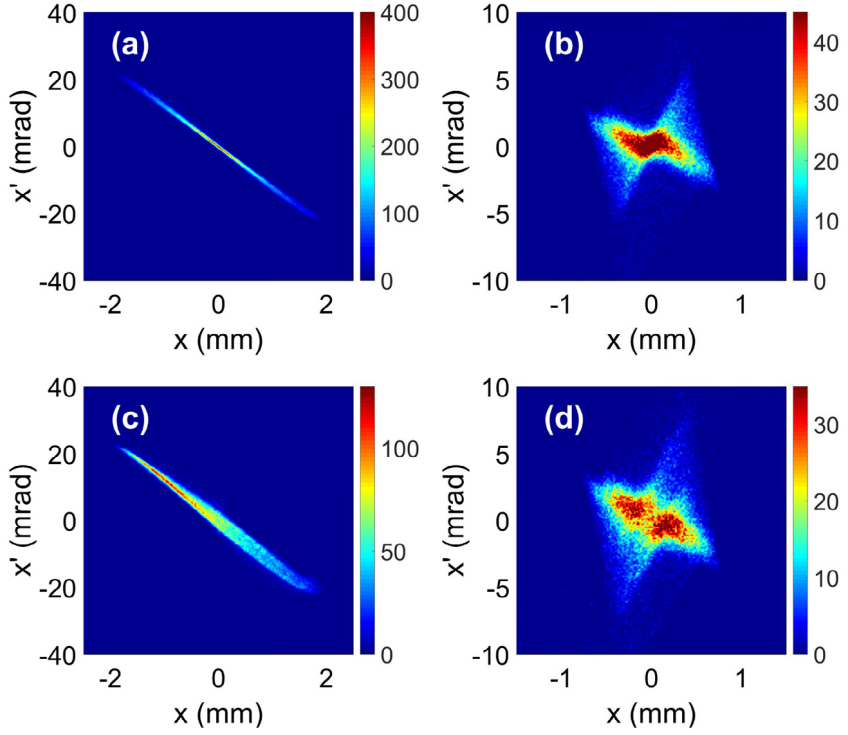

Fig. 7. Horizontal phase space of the beam at the input coupler section. Top: on-axis simulation; bottom: off-axis simulation with −4.5 mm booster structure offset. Solenoid current: (a, c) 175 A, and (b, d) 185 A.

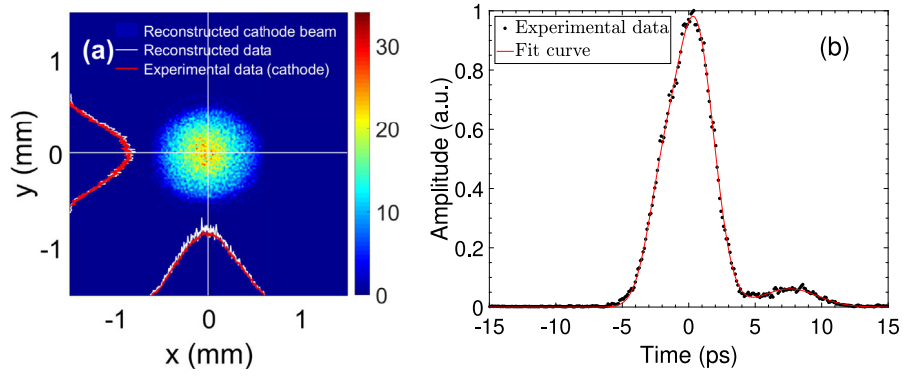

Fig. 8. Initial transverse beam distribution at the cathode (a) and longitudinal profile of the UV laser pulse (b). Intensity of the UV laser is normalized.

Despite the time constraints of beam delivery for acceleration experiments, systematic beam commissioning measurements were successfully performed with the electron injector. These measurements were compared with intensive beam dynamics modeling using ASTRA. A maximum number of measured input parameters was used to reproduce the experimental results. There was good overall agreement, giving

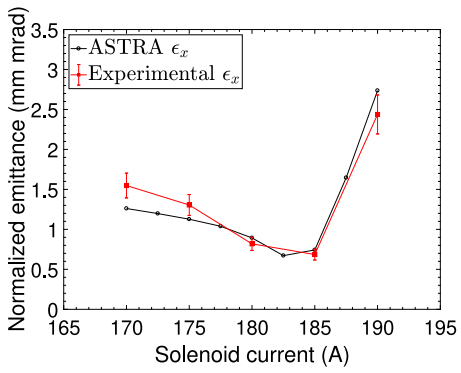

Fig. 9. Horizontal normalized emittance measured at the BTV 430042 screen compared to simulations.

us confidence in our injector model. To improve the agreement even further, two main parameters were identified; a potentially large misalignment in the booster structure and a tendency for a shorter initial bunch length, as originally anticipated. Recent UV pulse measurement confirmed that the actual measured pulse length was shorter than that predicted by the simulations. Correcting the alignment of the beam through the booster structure for each solenoid setting improved the emittance and resulted in a good agreement compared to simulations assuming an on-axis beam. The next step for AWAKE is to inject a very short bunch of 200 fs with a matched beta-function and bunch charge to load the wakefield into the plasma. The goal will be to demonstrate emittance preservation and a low energy spread at the end of the plasma acceleration. This challenging task requires a new injector, which is currently under design. The good agreement between the simulations and measurements for the current injector gives us confidence that our setup can be used in future work.

Declaration of competing interest

The authors declare that they have no known competing financial interests or personal relationships that could have appeared to influence the work reported in this paper.

CRediT authorship contribution statement

S.-Y Kim: Formal analysis, Writing - original draft, Visualization. **S. Doebert:** Conceptualization, Writing - original draft, Writing - review & editing, Supervision, Funding acquisition. **O. Apsimon:** Resources. **R. Apsimon:** Resources. **G. Burt:** Resources. **M. Dayyani:** Formal analysis. **S. Gessner:** Resources,Project administration. **I. Gorgisyan:** Resources. **E. Granados:** Resources,Visualization. **S. Mazzoni:** Resources. **J.T. Moody:** Resources. **M. Turner:** Resources. **B. Williamson:** Resources. **M. Chung:** Writing - Review & Editing, Supervision, Funding acquisition.

Acknowledgments

This work was partly supported by the National Research Foundation of Korea (Grants No. NRF-2016R1A5A1013277, No. NRF-2019R1F1A1062377, and NRF-2016-Fostering Core Leaders of the Future Basic Science Program/Global Ph.D. Fellowship Program).

References

[1] A. Caldwell, et al., Path to AWAKE: Evolution of the concept, Nucl. Instrum. Methods Phys. Res. A 829 (2016) 3–16, http://dx.doi.org/10.1016/j.nima.2015.12.050.
[2] E. Gschwendtner, AWAKE, a particle-driven plasma wakefield acceleration experiment, CERN Yellow Rep. 1 (2016) 271, http://dx.doi.org/10.5170/CERN-2016-001.271.
[3] J.M. Dawson, Nonlinear electron oscillations in a cold plasma, Phys. Rev. 113 (2) (1959) 383, http://dx.doi.org/10.1103/PhysRev.113.383.
[4] P. Muggli, et al., AWAKE Readiness for the study of the seeded self-modulation of a 400 GeV proton bunch, Nucl. Instrum. Methods Phys. Res. A 60 (1) (2017) 014046, http://dx.doi.org/10.1088/1361-6587/aa941c.
[5] M. Hüther, P. Muggli, Seeding of the self-modulation in a long proton bunch by charge cancellation with a short electron bunch, Nucl. Instrum. Methods Phys. Res. A 909 (2018) 67–70, http://dx.doi.org/10.1016/j.nima.2018.02.084.
[6] W. Lu, et al., Limits of linear plasma wakefield theory for electron or positron beams, Phys. Plasmas 12 (6) (2005) 063101, http://dx.doi.org/10.1063/1.1905587.
[7] K. Lotov, Physics of beam self-modulation in plasma wakefield accelerators, Phys. Plasmas 22 (10) (2015) 103110, http://dx.doi.org/10.1063/1.4933129.
[8] K. Pepitone, et al., The electron accelerators for the AWAKE experiment at CERN—baseline and future developments, Nucl. Instrum. Methods Phys. Res. A 909 (2018) 102–106, http://dx.doi.org/10.1016/j.nima.2018.02.044.
[9] J.S. Schmidt, et al., Status of the proton and electron transfer lines for the AWAKE Experiment at CERN, Nucl. Instrum. Methods Phys. Res. A 829 (2016) 58–62, http://dx.doi.org/10.1016/j.nima.2016.01.026.
[10] M. Turner, et al., External electron injection for the AWAKE experiment, in: 2018 IEEE Advanced Accelerator Concepts Workshop, AAC, 1–4, http://dx.doi.org/10.1109/AAC.2018.8659402.
[11] E. Adli, et al., Acceleration of electrons in the plasma wakefield of a proton bunch, Nature 561 (363) (2018) 7723, http://dx.doi.org/10.1038/s41586-018-0485-4.
[12] M. Turner, et al., Experimental observation of plasma wakefield growth driven by the seeded self-modulation of a proton bunch, Phys. Rev. Lett. 122 (5) (2019) 054801, http://dx.doi.org/10.1103/PhysRevLett.122.054801.
[13] E. Adli, et al., Experimental observation of proton bunch modulation in a plasma at varying plasma densities, Phys. Rev. Lett. 122 (5) (2019) 054802, http://dx.doi.org/10.1103/PhysRevLett.122.054802.
[14] A. Caldwell, et al., AWAKE Design report: a proton-driven plasma wakefield acceleration experiment at CERN, Technical report, 2013.
[15] P. Muggli, The AWAKE proton-driven plasma wakefield experiment at CERN, in: 6th Int. Particle Accelerator Conf. (IPAC'15), Richmond, VA, USA, May 3–8, 2015, pp. 2502–2505, http://dx.doi.org/10.18429/JACoW-IPAC2015-WEPWA007.
[16] O. Mete, et al., Production of long bunch trains with 4.5uC total charge using a photo injector, Phys. Rev. Accelerators Beams 15 (2012) 022803, http://dx.doi.org/10.1103/PhysRevSTAB.15.022803.
[17] O. Mete, et al., Modeling of an electron injector for the AWAKE project, in: 6th Int. Particle Accelerator Conf. (IPAC'15), Richmond, VA, USA, May 3–8, 2015, pp. 1762–1764, http://dx.doi.org/10.18429/JACoW-IPAC2015-TUPJE059.
[18] V. Fedosseev, et al., Generation and delivery of an ultraviolet laser beam for the RF-photoinjector of the awake electron beam, in: 10th Int. Partile Accelerator Conf. (IPAC'19), Melbourne, Australia, 19–24 May 2019, pp. 3709–3712, http://dx.doi.org/10.18429/JACoW-IPAC2019-THPGW054.
[19] S. Liu, et al., Development of the AWAKE stripline BPM electronics, in: International Conference on Technology and Instrumentation in Particle Physics, 2017, pp. 237–242.
[20] K. Floettmann, A space charge tracking algorithm, 1997, http://www.desy.de/~mpyflo/.
[21] K. Floettmann, Note on the thermal emittance of electrons emitted by Cesium Telluride photo cathodes, Technical report, 1997.
[22] D.H. Dowell, J.F. Schmerge, Quantum efficiency and thermal emittance of metal photocathodes, Phys. Rev. Special Topics 12 (7) (2009) 074201, http://dx.doi.org/10.1103/PhysRevSTAB.12.074201.
[23] K. Floettmann, ASTRA Manual Version 3.2, 2017.
[24] O. Apsimon, B. Williamson, A numerical approach to designing a versatile pepper-pot mask for emittance measurement, Nucl. Instrum. Methods Phys. Res. A 943 (2019) 162485, http://dx.doi.org/10.1016/j.nima.2019.162485.